OSU - ONR TR 83-7

UNDERSEA SOUND SPEED AND RANGE ESTIMATION

C.S. Hwang and R.R. Mohler
Department of Electrical and Computer Engineering
Oregon State University
Corvallis, Oregon 97331

Prepared for

The Office of Naval Research
under
Contract No. N00014-81-K0814
R.R. Mohler, Principal Investigator

ON UNDERSEA SOUND SPEED AND RANGE ESTIMATION[1]

C.S. Hwang and R.R. Mohler[2]

Abstract

Estimation of an acoustic wave velocity in the ocean and its utilization to improve object localization are studied here.

Time delay and/or Doppler shift are measured by the vertically deployed sensors in two-dimensional systems. Various sensor configurations (up to three sensors) are considered. The information rate grows very fast when the measurement equation includes Doppler shift (1D1P, 2D1P). The system is totally unobservable with one sensor (1D), but the system is observable when two or three are employed. Three-sensor, two-delay, one Doppler (2D1P) measurement gives the strongest observability.

Several variations of Extended Kalman Filter (EKF) algorithms are tried.

Approximated expression of the measurement equation with three sensors (2D1P) shows the best velocity estimation performance.

With this estimated sound velocity, target range is compared with the nonestimated case. As the measurement noise level increases, tracking performance of the estimated case becomes superior to the nonestimated case.

---

[1]Research supported by ONR Contract No. N00014-81-K-0814 and NUWES Contract No. N00408-82-D-0675.

[2]Author's address: Department of Electrical and Computer Engineering, Oregon State University, Corvallis, OR 97331. During August 1983 to July 1984, the authors are at the Department of Electrical Engineering, Naval Postgraduate School, Monterey, CA 93940. R.R. Mohler is an IEEE Fellow.

1.0 INTRODUCTION

The object here is to study recursive estimation of sound velocity in sea water and its use in improved object localization. It is well known that sound velocity can vary quite significantly as a function of depth, salinity, temperature and weather - especially in coastal inlets. Sound velocity in seawater is very significant to ascertain the distance between two points which is obtained by just multiplying the time delay between them. Practically, two devices-- a velocity meter and bathythermograph (XBT), are commonly used for finding the velocity of the sound propagation in the water.

In [1], indirect measurement of the average velocity is studied by searching for the ray path which may be experienced with measured time delay betweent two points. Velocity at a specific layered depth is stored in computer memory for reference.

In this paper, an attempt is made to estimate sound velocity by using the Extended Kalman Filter (EKF) algorithm and its variations with various measurement configurations. By adding more sensors, up to three, observability of the system is improved.

Since this observability for highly nonlinear measurement equations has not been solved, the equations are first linearized and then the information matrix and information-rate matrix are obtained. Tests of the singularity of the information matrix shows that three sensors with three measurements (two delays, one Doppler) makes the system fully observable after the first measurement data arrived for the two-dimensional tracking system. Time propagation of the eigenvalue of the information - rate matrix, also shows that two-delay, one-Doppler measurement, gives the fastest learning about the system. Here, the sensor deployment is assumed to be vertical in depth.

Since the system equations are linear and the measurement equations are nonlinear with discrete observation, a discrete-type EKF with Gaussian sequence noises in both system and measurement is simulated.

2.0 SENSOR CONFIGURATION AND MEASUREMENT

For good measurement and system observability, sensor configuration is very important. Even with the same number of sensors and the same deployment structures, different quantities can be measured. We can measure absolute time delay or time delay difference of two sensors, Doppler or Doppler difference, or any combination thereof.

Each of these measurement policies provide different information about system states due to the different degree of observability, but also, it is desired to know the minimum number of sensors which gives just enough information to estimate certain state variables. Here, several alternatives of sensor and target configurations, when the target moves with constant velocity along the ocean surface are considered.

Figure 1 shows sensor and target configuration for up to three sensors in a straight vertical array.

In the one-sensor case, only absolute time delay or absolute Doppler shift between T and s_2 can be measured. Here T and s_2 need to be synchronized to observe those quantities, i.e., effective for active SONAR. Another problem here is poor observation of state; actually the system was unobservable with absolute time delay measurement during the first five minutes of the observation period.

The two-sensor case is much better, i.e., either absolute quantities or comparative difference of delay or Doppler can be measured. Also, active or passive systems may be used. Another advantage of this configuration is the magnitude of observed quantities. When target T approaches the sensor array, closer and closer, the actual magnitude of the comparative delay t_{12} or Doppler f_{12} becomes larger and larger. This is because sensors s_1, s_2 are

1). One-sensor

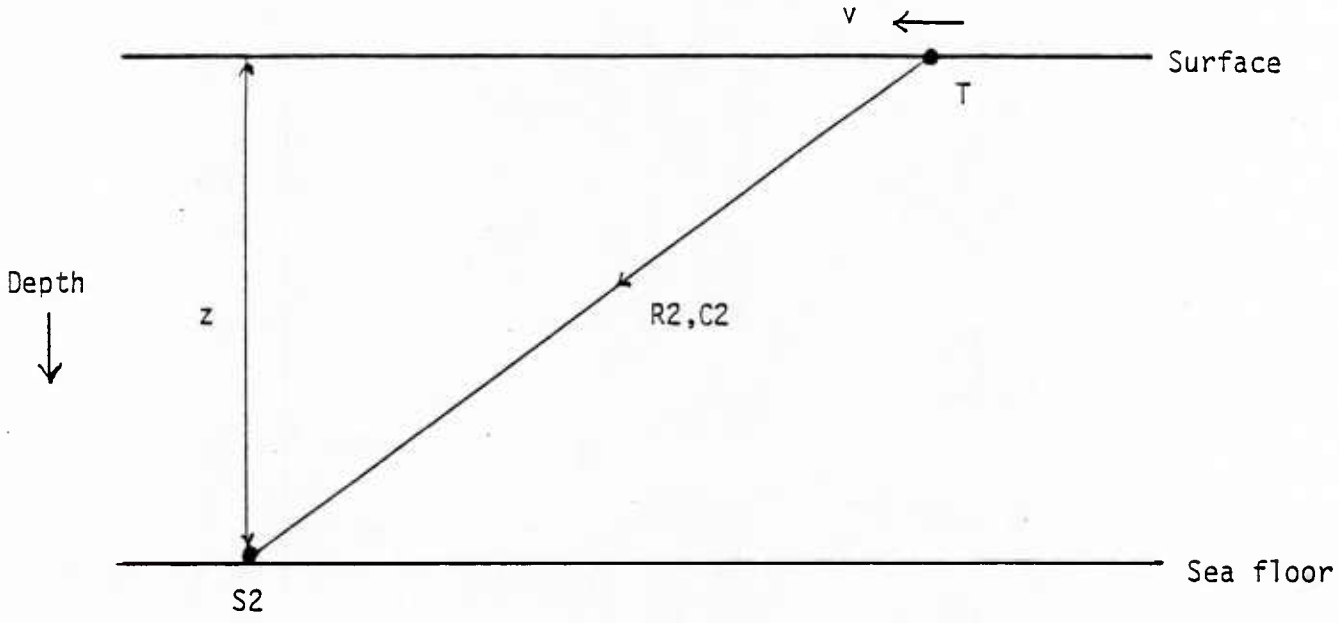

2). Two-sensor

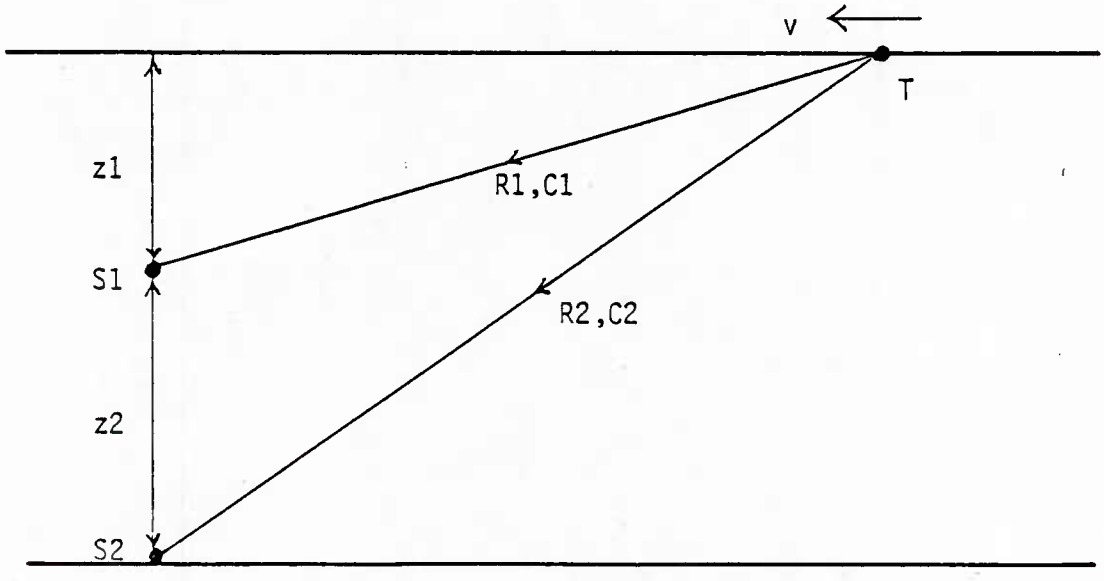

3). Three-sensor

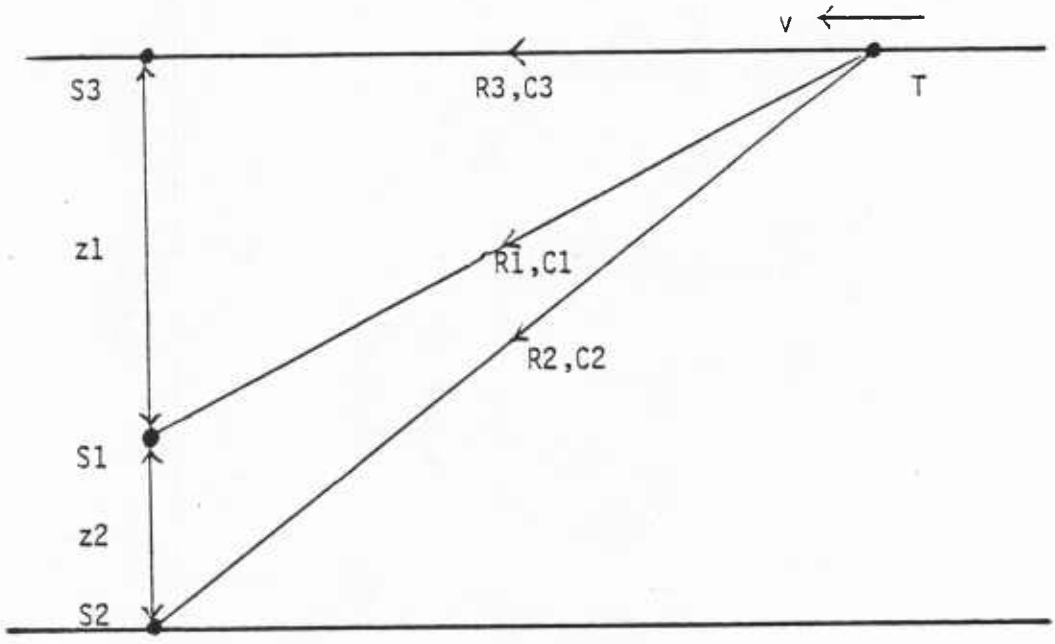

Figure 1, Sensor configuration

located below the target vertically. But when the target locates between the sensors, then the measured quantities t_{12}, D_{12} may be very small thus resulting in poor observation. If T locates exactly halfway between the two sensors the t_{12}, f_{12} would be identically zero during such time, so that an unobservable system results, again. Even so, it will be seen that the above cases may not be fully observable with t_{12} and f_{12} measurements.

So, in the third figure, one more sensor s_3 is added at the surface plane. With this deployment several possible measurements are considered as follows:

a) Two delay differences t_{12}, t_{13};

b) Three delay differences t_{12}, t_{13}, t_{23};

c) Two delay differences t_{12}, t_{13}; and one Doppler difference f_{12}.

In this three-sensor system, observability is improved much compared to the first two cases. But Cases a and b exhibit somewhat poor observability during the first several observation periods. However, with Case c the system is fully observable after the first measured data arrived and the observability is very strong compared to the first two cases. Consequently, Case c is chosen for the measurement equation in the simulation of the two-dimensional system shown.

3.0 SYSTEM MODEL

In a two-dimensional coordinate system, at least four state variables are required to describe the motion of the point target, i.e., target position and its velocity in each coordinate. To involve the acoustic velocity in the system model, consider the velocity along the direct path from the source (target) to the sensors as another state variable. But to reduce the number of state variables, assume the surface acoustic velocity C_3 is a known constant value for the three-sensor case. By assuming the origin is at s_2, define the state variables as follows:

x_1 is target position in x-direction

x_2 is target velocity in x-direction

x_3 is target position in y-direction

x_4 is target velocity in y-direction

x_5 is C_1 (acoustic wave velocity in R_1)

x_6 is C_2 (acoustic wave velocity in R_2)

With the above definition, the discrete type system equation can be written as

$$x(k+1) = \begin{bmatrix} 1 & \Delta T & 0 & 0 & 0 & 0 \\ 0 & 1 & 0 & 0 & 0 & 0 \\ 0 & 0 & 1 & \Delta T & 0 & 0 \\ 0 & 0 & 0 & 1 & 0 & 0 \\ 0 & 0 & 0 & 0 & 1 & 0 \\ 0 & 0 & 0 & 0 & 0 & 1 \end{bmatrix} x(k) + W(k) \ ,$$

where $x(0) = x_0$, ΔT is the sampling interval, and $W(k)$ is a white Gaussian noise sequence with covariance

$$Q(k) = E[W(k)\ W(k)^T]$$

$$= \begin{bmatrix} \sigma_x^2 & & & & & & \\ & \sigma_{v_x}^2 & & & & 0 & \\ & & \sigma_y^2 & & & & \\ & & & \sigma_{v_y}^2 & & & \\ & & & & \sigma_{C_1}^2 & & \\ 0 & & & & & & \sigma_{C_2}^2 \end{bmatrix} .$$

The basic measuring quantities are time delay difference t_{ij} between sensors and Doppler frequency difference f_{ij} from carrier frequency $f_c = 3500$ Hz, which seems widely used in practical SONAR systems. So, for example, when three sensors are used in the measurement system with two delays and one Doppler (2D1P), the observation equation becomes

$$y(k) = \begin{bmatrix} \text{delay difference between } s_1 \text{ and } s_2 \\ \text{Doppler differnce between } s_1 \text{ and } s_2 \\ \text{Delay difference between } s_1 \text{ and } s_3 \end{bmatrix} +$$

{measurement noise}

$$= \begin{bmatrix} t_{12}(k) \\ f_{12}(k) \\ t_{13}(k) \end{bmatrix} + V(k) ,$$

$$= \begin{bmatrix} \frac{R_2(k)}{C_2(k)} - \frac{R_1(k)}{C_1(k)} \\ f_c\left(\frac{\dot{R}_2(k)}{C_2(k)} - \frac{\dot{R}_1(k)}{C_1(k)}\right) \\ \frac{R_2(k)}{C_2(k)} - \frac{R_3(k)}{C_3} \end{bmatrix} + V(k) \quad ,$$

$$= \begin{bmatrix} \frac{(x_1^2 + x_3^2)^{1/2}}{x_6} - \frac{(x_1^2 + (x_3 - z_2)^2)^{1/2}}{x_5} \\ \frac{f_c(x_1x_2 + x_3x_4)}{x_6(x_1^2 + x_3^2)^{1/2}} - \frac{f_c(x_1x_2 - (x_3 - z_2)x_4)}{x_5(x_1^2 + (x_3 - z_2)^2)^{1/2}} \\ \frac{(x_1^2 + x_3^2)^{1/2}}{x_6} - \frac{x_1}{C_3} \end{bmatrix} + V(k) \quad ,$$

$$= h(x(k)) + V(k) \quad ,$$

Where V(k) is assumed independent with x(0) and W(k) white Gaussian noise with covariance

$$R(k) = E[V(k)\ V(k)^T] \quad ,$$

$$= \begin{bmatrix} \sigma_{t_{12}}^2 & & 0 \\ & \sigma_{f_{12}}^2 & \\ 0 & & \sigma_{t_{13}}^2 \end{bmatrix} \quad ,$$

The other cases of observation equations have a similar form, but measure different quantities. For comparison of observability of the system and filtering performance possible observation equations are given below.

1) One-Sensor (1). of Fig. 1); 1S(1D)

$$h(x(k)) = \text{one absolute time delay between T and } s_2$$
$$= R(k)/C(k)$$

2) Two-Sensor (2). of Fig. 1); 2s(1D1P),

$$h(x(k)) = \begin{bmatrix} t_{12}(k) \\ f_{12}(k) \end{bmatrix} .$$

3) Three-Sensor (3) of Fig. 1)

- 3s(2D)

$$h(x(k)) = \begin{bmatrix} t_{12}(k) \\ t_{13}(k) \end{bmatrix} .$$

- 3s(3D)

$$h(x(k)) = \begin{bmatrix} t_{12}(k) \\ t_{13}(k) \\ t_{23}(k) \end{bmatrix} .$$

In any case, the system equations are simple linear ones, but the observation equations are nonlinear.

4.0 OBSERVABILITY OF THE SYSTEM

Generally, increased system observability improves the quality of an estimate and speeds up the convergence of estimations. Also, some redundant observation is desired to reduce adverse effects of measurement errors.

Since the system has special nonlinear structure with any considered measurement equations, it is necessary to know which measuring policy is the "best" one. The meaning of "best" here is that which requires a minimum number of sensors to maintain an observable system.

Many investigations have been conducted of nonlinear-system observability. Most of them, for example, Kostyukovskii [8,9], Tarn, et al. [10], Griffith [11], Fitts [12], Fujisawa [13] and Schoenwandt [14], tried to find a method to check if the observed or measured data is enough to decide every initial state x(0) uniquely, i.e., somehow to check unique connectedness of measurement and system state using a nonlinear mapping concept or by extending the well known rank test. Unfortunately, both of the above concepts are very difficult to apply directly here because the measurement equations involve complicated nonlinear expressions in their denominator.

Here, the system is modified and then the observability matrix testing concepts are applied. This method is suggested by Jazwinski [5] when system noises are small.

First, the measurement equation is linearized about the most recently estimated value $\hat{x}(k)$, i.e.,

$$y(k+1) = h(x(k)) + V(k)$$

$$\approx H(\hat{x}(k))x(k) + V(k).$$

Then, with the system equation

$$x(k + 1) = A(k + 1, k)x(k) + B(k)W(k),$$

the information matrix I(k,1) is

$$I(k, 1) \triangleq \sum_{i=1}^{k} A^T(i, k)H^T(\hat{x}(i))R(i)^{-1}H(\hat{x}(i))A(i, k).$$

This is a completely analogous definition of the observability matrix for the continuous dynamic system with

$$I(t,t_0) \triangleq \int_{t_0}^{t} A^T(\tau,t)H^T(\hat{x}(\tau))R(\tau)^{-1}H(\hat{x}(\tau))A(\tau,t)dt \ .$$

After some algebra, the iterative algorithm to compute time propagation of I(k + 1, 1) becomes

$$I(k + 1, 1) = A^T(k, k + 1)\ I(k,1)\ A(k, k + 1)$$

$$+ H^T(\hat{x}(k + 1))R^{-1}(k + 1)\ H(\hat{x}(k + 1)) \ ,$$

$$I(1, 1) = 0 \ .$$

Then the discrete system is said to be completely observable with respect to observations

$$\{y_1, y_2, \ldots\ldots, y_k\}$$

if, and only if the information matrix $I(\cdot)$ is positive definite, i.e.,

$$I(k, 1) > 0, \text{ for some } k > 1.$$

The second term of $I(\cdot)$, i.e.,

$$H^T(\hat{x}(k))R^{-1}H(\hat{x}(k))$$

is known as the information-rate matrix which shows how fast the filter obtains information from the measurement equation.

Before positive definiteness of $I(\cdot)$ is checked, i.e., the observability of the system, consider the eigenvalue of this information rate matrix. Of course, the larger its eigenvalue implies the faster the observation gains information or learns about the state. Table 1 shows the eigenvalue ($\lambda 6$) corresponding to x_6 of this matrix for different measurement equations considered before. This shows that the information rate of the three-sensor, two-delay measurement (3s(2D)) and three-sensor, three-delay (3s(3D)) are almost the same. And 2s(1D1P) and 3s(2D1P), also, grow at almost the same rate in spite of the different number of sensors. The magnitude differs tremendously, i.e., the information rate in cases with Doppler measurements is much larger (almost 200 times). So, it is suggested that Doppler measurements are very useful here. System 1s(1D) is far inferior to the other measurement configuration.

Another interesting fact is that when only time delay is measured corresponding to the first three columns of Table 1, the information rate is decreasing with increasing time. On the other hand, when Doppler as well as

Table 1. Eigenvalue (λ_6) of Information Rate Matrix $(H^T R^{-1} H)$

Time \ Meas.	1s(1D)	3s(2D)	3s(3D)	2s(1D1P)	3s(2D1P)
t = 1 min.	.00014	.060	.064	2.6	2.7
2	.00012	.076	.080	3.9	3.8
3	.00010	.059	.062	5.5	5.4
4	.00008	.044	.047	8.4	8.3
5	.00007	.035	.038	12.2	12.3

delay is measured, the rate increases with time. This also suggests that Doppler must be a measured quantity.

Next the observability of the above measurement equations are compared by computing the singularity of the information matrix I(k, 1). Table 2 shows this result. As expected, with one-sensor, one-delay (1s(1D)) measurement, the system is unobservable during the whole five minutes of observation. In the next three cases, 2s(1D1P), 3s(2D), 3s(3D), the system is observable after 0.5 min. from the beginning of estimation which corresponds to after the second measured data arrived. The magnitudes, determinants of the information matrix, are very small here, but increasing with time. At the final time t = 5 min. the strength of the observability is much different depending on the measurement policy. However, most strong observability occurs from the last measurement case, 3s(2D1P). Here, the system is observable from just after the first measurement data is done. And, also, the magnitude is much larger than the other cases. At the final time, the strength of nonsingularity is almost 20 times larger than that of 3s(3D).

Within the limited measurement systems considered here, the comparison shows that the observability of the system is a strong function of the number of sensors as would be expected. For system observability from within one or two measurements, at least three sensors are needed. If we employ the 3s(2D1P) policy, the system is completely observable from the first measurement on.

Table 2. Observability (Singularity of Information Matrix)

Meas. Time	1s(1D)	3s(2D)	3s(3D)	2s(1D1P)	3s(2D1P)
0 min.					5.33×10^{-17}
0.5		4.88×10^{-21}	8.13×10^{-22}	3.8×10^{-21}	
1.0					
1.5					
2.0					
2.5	Unobservable	3.98×10^{-15}	2.56×10^{-11}	2.0×10^{-10}	1.08×10^{-9}
3.0					
3.5					
4.0					
4.5					
5.0		3.73×10^{-9}	7.63×10^{-8}	6.3×10^{-7}	1.24×10^{-5}

5.0 EKF AND ITS VARIATIONS

Here, the system equation is linear in the state, but the measurement equation is not, so the usual Kalman-Bucy filter cannot be directly applied. Hence, a discrete-type EKF algorithm is studied. Its recursive computational steps can be described as follows:

1) Given $\hat{x}(k, k)$, $P(k,k)$ from the previous estimation with initial values $\hat{x}(0, 0)$, $P(0, 0)$.

2) $\hat{x}(k + 1, k) = A(k + 1, k)\hat{x}(k, k)$, predicted state estimation.

3) $P(k + 1, k) = A(k + 1, k)P(k, k)A^T(k)$, predicted error covariance.

4) $K(k + 1) = P(k + 1, k)H^T(k + 1)\left[H(k + 1)P(k + 1, k)H^T(k + 1) + R(k)\right]^{-1}$, gain matrix.

5) $\hat{x}(k + 1, k + 1) = \hat{x}(k + 1, k) + K(k + 1)\left[y(k + 1) - h(\hat{x}(k + 1, k))\right]$, new state estimation.

6) $P(k + 1, k + 1) = \left[I - K(k + 1)H(k + 1)\right]P(k + 1, k)$,
or $= \left[I - K(k + 1)H(k + 1)\right]P(k + 1, k)\left[I - K(k + 1)H(k + 1)\right]^T + K(k + 1)R(k)K^T(k + 1)$, new error covariance matrix.

7) Repeat from Step 1) with $k + 1 \rightarrow k$,

where $H(k + 1) = \left.\frac{\partial h(x)}{\partial x}\right|_{x = \hat{x}(k + 1, k)}$.

The EKF is modified for the simulation purpose as below. This was done to be more useful or to have better characteristics for the stated problem.

a) EKF with Exact Expression of H Matrix.

From the results of the previous section, it is seen that the system is fully observable with 3s(2D1P) measurements. Consequently, several EKF variations for this measurement equation are compared with

$$R_1(k) = \left(x_1^2 + (x_3 - z_2)\right)^{1/2} ,$$

$$R_2(k) = \left(x_1^2 + x_3^2\right)^{1/2} ,$$

$$h(x(k)) = \begin{bmatrix} \dfrac{R_2}{x_6} - \dfrac{R_1}{x_5} \\ \dfrac{f_c(x_1x_2 + x_3x_4)}{x_6R_2} - \dfrac{f_c(x_1x_2 - (x_3 - z_2)x_4}{x_5R_1} \\ \dfrac{R_2}{x_6} - \dfrac{x_1}{C_3} \end{bmatrix} ,$$

$$H(k+1) = \frac{\partial h}{\partial x}\Big| x = \hat{x}(k+1, k) ,$$

$$= \begin{bmatrix} \dfrac{x_1}{x_6R_2} - \dfrac{x_1}{x_5R_1}, & 0 & , \dfrac{x_3}{R_2x_6} - \dfrac{x_3 - z_2}{R_1x_5}, & 0 & , \dfrac{R_1}{x_5^2}, & \dfrac{-R^2}{x_6^2} \\ H_{21} & , \dfrac{-f_cx_1}{R_1x_5} + \dfrac{f_cx_1}{R_2x_6}, & H_{23} & , \dfrac{f_cx_3}{R_2x_5} - \dfrac{f_c(x_3 - z_2)}{R_1x_5}, & H_{25}, & H_{26}, \\ \dfrac{x_1}{x_6R_2} - \dfrac{1}{C_3} & , & 0 & , \dfrac{x_3}{x_6R_2}, & 0 & , 0 , \dfrac{-R_2}{x_6^2}, \end{bmatrix}_{x = \hat{x}(k+1,k)}$$

where

$$H_{21} = -f_c\left(\frac{x_2}{x_5}\right)\left(\frac{1}{R_1} - \frac{x_1^2}{R_1^3}\right) + f_c\left(\frac{x_2}{x_6}\right)\left(\frac{1}{R_2}\right)\left(\frac{1}{R_2} - \frac{x_1^2}{R_2^3}\right) - \frac{f_cx_1x_3x_4}{x_6R_2^3} + \frac{f_cx_1(x_3 - z_2)x_4}{x_5R_1^3},$$

$$H_{23} = \frac{f_cx_4}{x_6}\left(\frac{1}{R_2} - \frac{x_3^2}{R_2^3}\right) - \frac{f_cx_4}{x_5}\left(\frac{1}{R_1} - \frac{(x_3 - z_2)^2}{R_1^2}\right) - f_c\frac{x_1x_2(z_2 - x_3)}{x_5R_1^3} - \frac{f_cx_1x_2x_3}{x_6R_2^3} ,$$

$$H_{25} = \frac{f_c x_1 x_2}{R_1 x_5^2} + \frac{f_c (x_3 - z_2) x_4}{R_1 x_5^2} ,$$

$$H_{26} = \frac{-f_c x_3 x_4}{x_6^2 R_2} - \frac{f_c x_1 x_2}{R_2 x_6^2} .$$

Since the H matrix involves high-order multiplication and division, a little error in estimation $\hat{x}(k+1, k)$ may cause a large computational error. This is further brought out by simulation. Therefore, a simplified alternate approximation of H was sought.

b) EKF with Simplified H Matrix.

Due to the complicated expression of the H matrix and insignificance of some terms in it, consider a simplified version of H without any appreciable deterioration of filter performance.

From the actual values of estimation used here

$$\hat{x}_3 \hat{x}_4 , \ (\hat{x}_3 - z_2)\hat{x}_4 \ll \hat{x}_1 \hat{x}_2 .$$

This is due to our special system structure, i.e., $\hat{x}_1$ is larger value on the other hand, $\hat{x}_4$ is close to zero. So the measurement matrix h(x) is approximated by

$$h(x) = \begin{bmatrix} \frac{R_2}{x_6} - \frac{R_1}{x_5} \\ \frac{f_c x_1 x_2}{x_6 R_2} - \frac{f_c x_1 x_2}{x_5 R_1} \\ \frac{R_2}{x_6} - \frac{x_1}{C_3} \end{bmatrix} .$$

Now the H matrix with this h has fairly good form which may involve less computational error.

With the approximated H, very good state estimation results, as can be seen from Figure 2.

c) EKF with Artificial Measurement Error Term.

Denham [4] indicated that when measurements are nonlinear and nonlinearity is comparable to measurement noise, filter performance can be improved by adding an artificial error covariance term R_{art} as

$$R_T = R + R_{art},$$

i.e., artificially increase the measurement-error covariance, but its effect is obvious from the expression

$$\hat{x}(k + 1, k + 1) = A(k + 1, k)\hat{x}(k + 1, k) + K[y(k + 1) - h(\hat{x})] ,$$

with

$$\text{gain} \quad K = PH^T[HPH^T + R_T]^{-1}$$

By increasing R_T, the gain K is decreased. The limiting case of the above is

$$R_T \to \infty, \quad K \to 0,$$

Figure 2 . Comparison of various EKF algorithms ($\hat{x}_1$)
(mean of 15 runs)

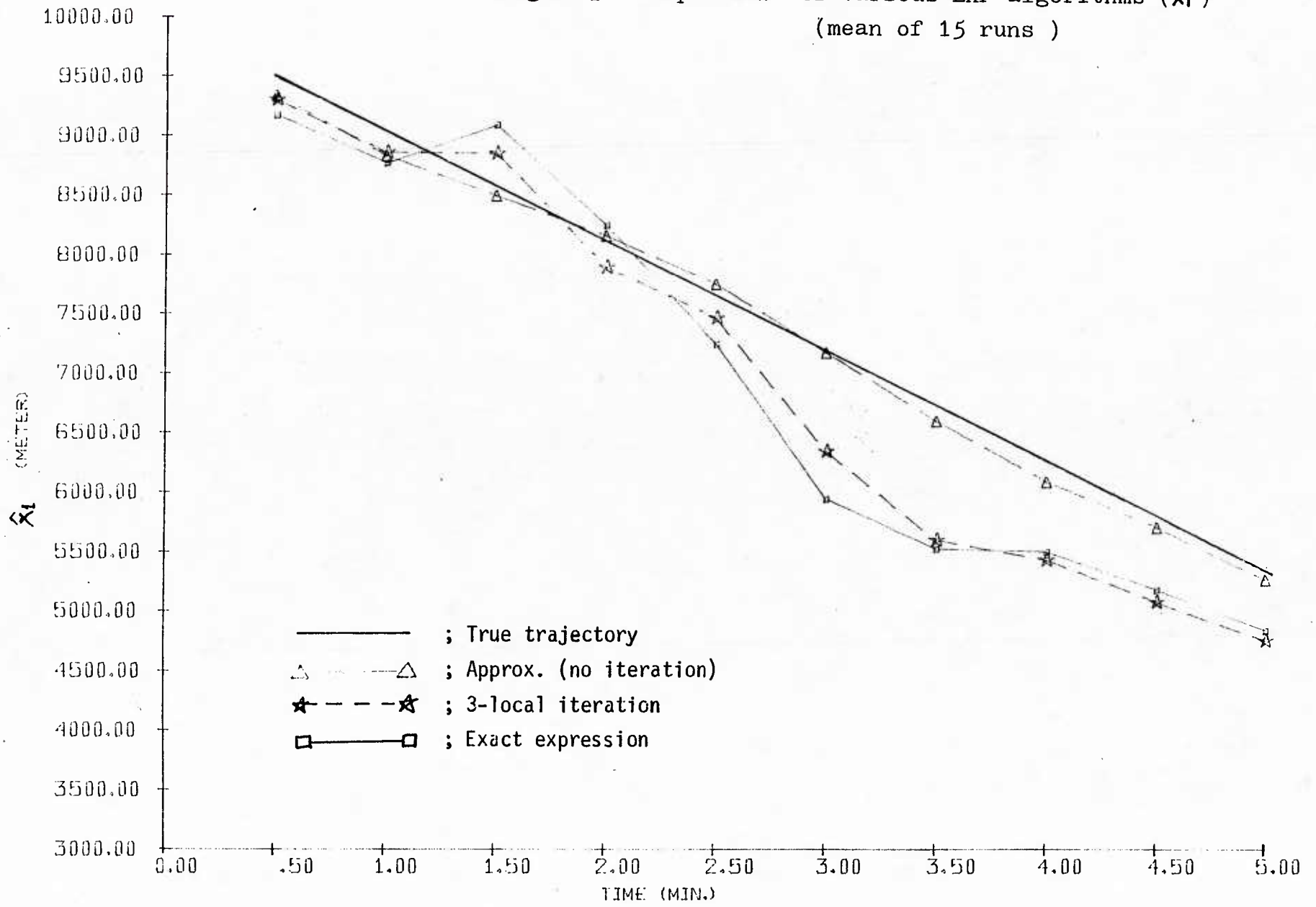

then

$$\hat{x}(k + 1, k + 1) = A(k + 1, k)\hat{x}(k + 1, k) \ ;$$

i.e., in the extreme limit nothing is learned from the measurement.

d) EKF with Local Iterations

With this algorithm the predicted state $\hat{x}(k + 1, k)$ is updated before calculating a new estimation $\hat{x}(k + 1, k + 1)$, i.e., iterates several more times (Step 4 and 5 in the original EKF) between measurements. See Denham [4] and Jazwinski [5].

Then the i-th iteration of N total iterations becomes

$$\eta_{i+1} = \hat{x}(k + 1, k) + K(\eta_i)[y(k + 1) - h(\eta_i) - H(\eta_i)(\hat{x}(k + 1, k) - \eta_i] \ ,$$

where

$$\eta_1 = \hat{x}(k + 1, k), \text{ and}$$

$$\eta_\ell = \hat{x}(k + 1, k + 1) \ , \text{ for } \ell = 2, \ldots, N.$$

This iteration repeats until improvement

$$(\hat{x}(k + 1, k) - \eta_i)$$

is small enough. At every iteration $K(\eta_i)$, $h(\eta_i)$ and $H(\eta_i)$ are recalculated, thus at the ℓ-th iteration, the new covariance $P(k + 1, k + 1)$ is computed and then waits for new measurement data, and so on.

This algorithm, obviously, has some advantages such as:

1) Effective use of processor or computer between sampling intervals,

2) Improving the state estimation by improving the reference state.

Unfortunately, there are several disadvantages such as:

a) Only useful when unobservable states are linear,

b) Accumulation of truncated error due to repeated iterations, and

c) Computational error may be accumulated, also.

Here, it does not seem to be useful as can be seen in Figure 2. This may be due to the particular nonlinear structure of the measurement equation, $h(x)$, which may nullify the anticipated advantages.

6.0 RESULTS

For comparison of different measurements, the following parameters are chosen:

ΔT = 15 sec. (measurement interval).

$\hat{x}(0)$ = initial condition of state variables,

$$= \begin{bmatrix} \hat{x}_1(0) = 10{,}000 \text{ m} \\ \hat{x}_2(0) = -15.433 \text{ m/s (30 knots; approaching to the sensor)} \\ \hat{x}_3(0) = 4000 \text{ m} \\ \hat{x}_4(0) = 0 \text{ m/s} \\ \hat{x}_5(0) = 1500 \text{ m/s} \\ \hat{x}_6(0) = 1500 \text{ m/s} \end{bmatrix}$$

$+ \sigma_i \times N(0, 1)$, $i = 1....6.$

where

$\sigma_1 = \sigma_x = 100$ m (1% of initial value of x_1)

$\sigma_2 = \sigma_{vx} = 0.15$ m/s (1%)

$\sigma_3 = \sigma_y = 40$ m (1%)

$\sigma_4 = \sigma_{vy} = 0.1$ m/s

$\sigma_5 = \sigma_{C_1} = 7.5$ m/s (0.5%)

$\sigma_6 = \sigma_{C_2} = 7.5$ m/s (0.5%).

The measurement noise assumed was zero mean white Gaussian with variances.

$\sigma_{t_{12}} = 0.038$ sec. (10% of the first measurement)

$\sigma_{f_{12}} = 0.1875$ Hz (10%),

$\sigma_{t_{13}} = 0.052$ (10%),

and

$f_c = 3500$ Hz (carrier frequency of modulation),

$z_1 = 2000$ m (intersensor distance of s_1 and s_3),

$z_2 = 2000$ m (intersensor distance of s_1 and s_2).

With the above parameters, 15 runs were averaged. Figure 3 shows the sound speed estimation along the range R_2 for the different measurement structures. Clearly, for the one- or two-sensor cases, the filtering function is not so good compared to the three-sensor case. The reason for the large bias from the true trajectory may be due to the lack of observability. Actually, these two cases showed poor observability as seen in Table 2 previously.

For three-sensor measurements, it is difficult to compare performance, but error covariances of this case show that the two-delay, one-Doppler meas-

Figure 3. Comparison of sound speed estimation ($\hat{x}_6$)
(mean of 15 runs)

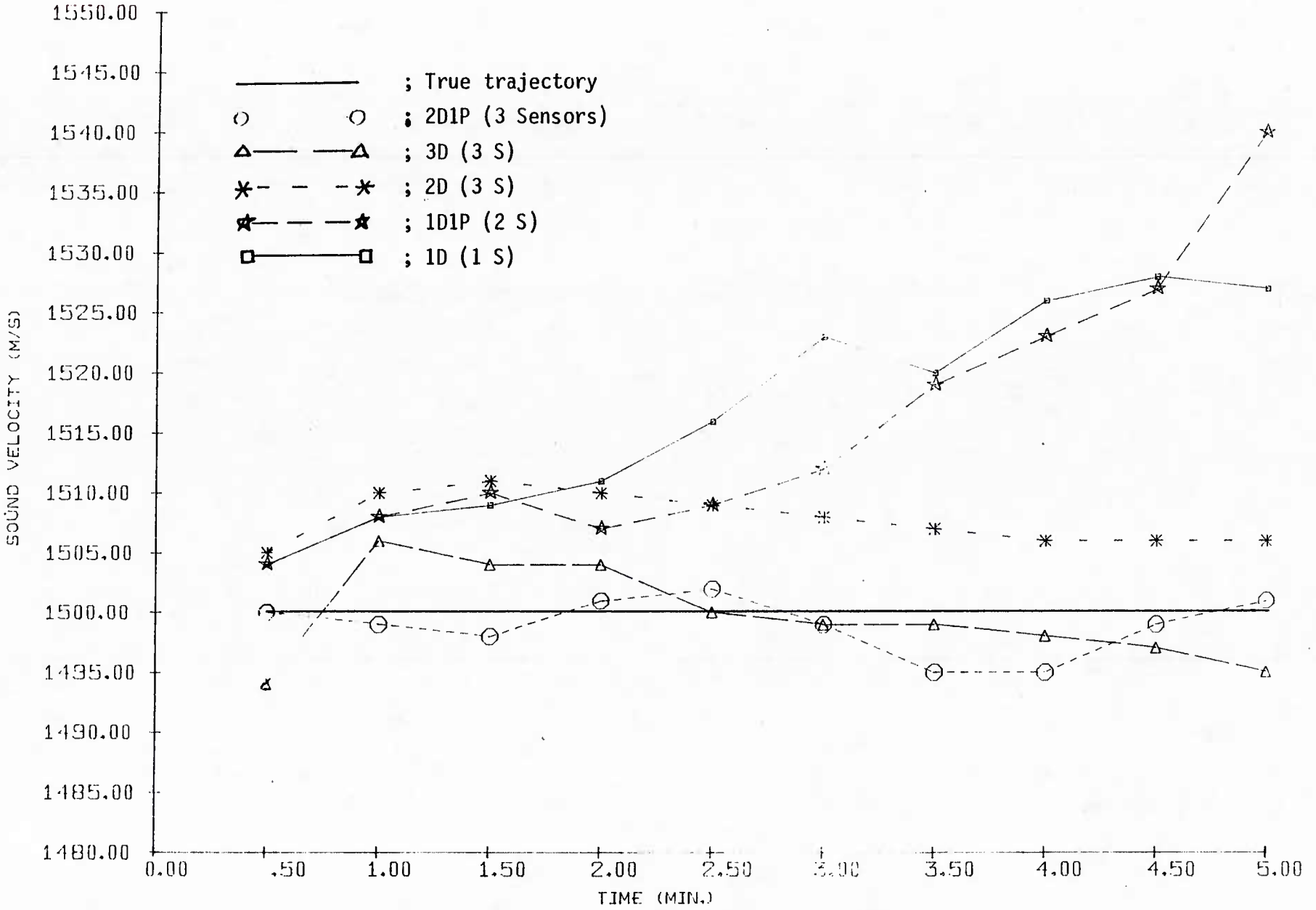

urement system (2D1P) has the smallest value at the final time. This is shown in Figure 4 and Table 3. For 3s(2D) and 3s(3D) measurements, the variances grow slowly, but for 3s(2D1P) they decrease steadily. So, it is concluded that for the two-dimensional system observability and good sound speed estimation requires at least three sensors. Further for best observability and best filtering performance, Doppler measurement which is combined with delay measurement is essential.

Next, improvement of the target range is examined by comparing "without sound velocity estimation" and "with estimation." For convenience, choose range R_2 which is a direct path from target to sensor at the sea floor (Figure 1). Since it is expected that the effects of the estimation or filtering effect will be most clear when the measurement noise level is high, the original 10% noise level is increased to 20%. The system noise level, also, is increased to 5% from its 1% level. Figure 5 shows this comparison for an average of 15 runs. Clearly, after about two minutes, the estimated range trajectory with 2D1P measurement policy shows smoother and more accurate trajectory than the one without estimated acoustic velocity.

To show more detailed effects of estimation as a function of measurement noise level, Figures 6 and 7 are provided. Noise levels chosen here are 5%, 10%, and 20%. When the noise level is low, for example 5%, the difference of range tracking performance is not so significant. However, when noise levels increase, the differences of performance become more significant.

Figure 4. Error covariance of $\hat{x}_6$

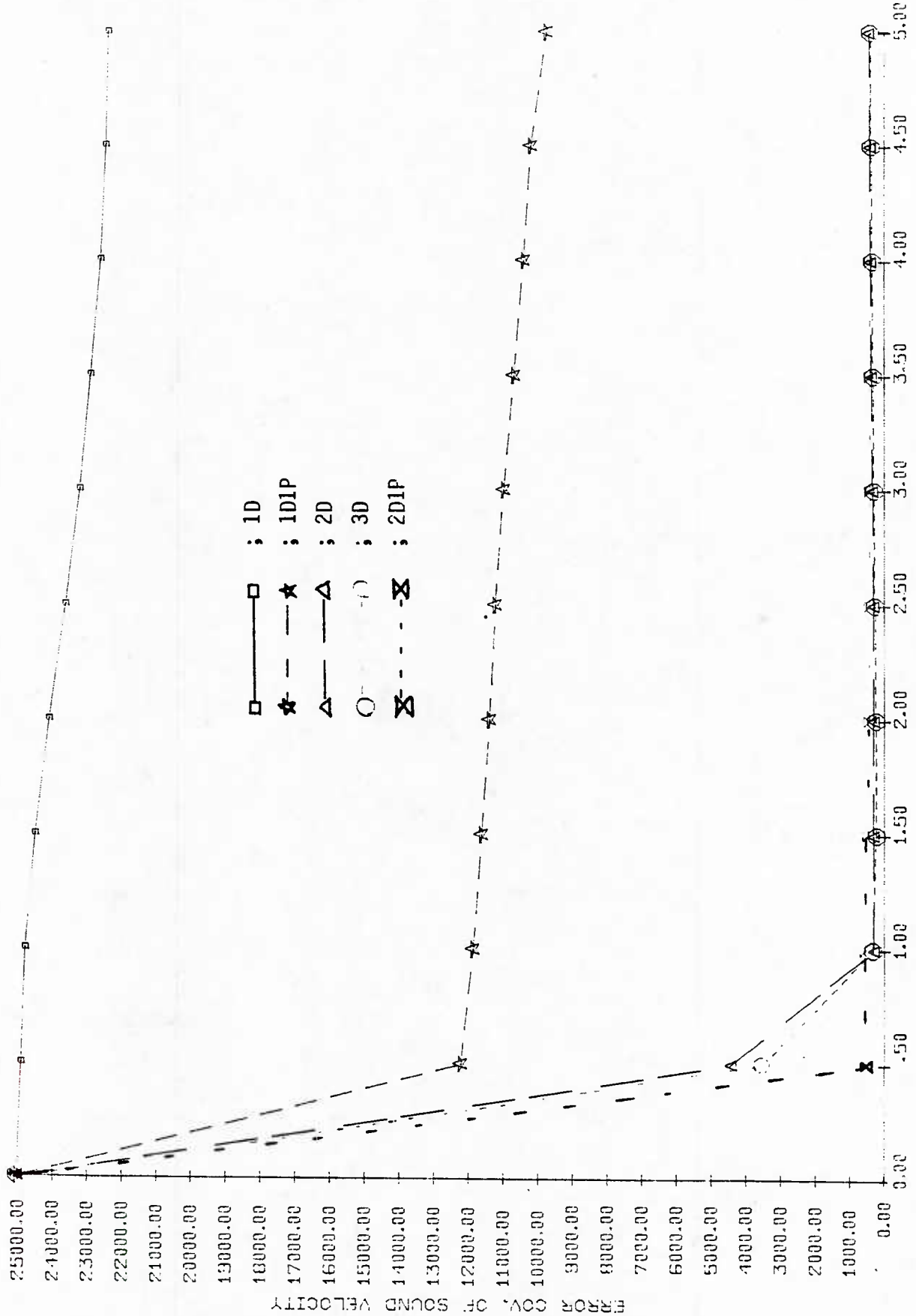

Table 3. Error Covariance of $\hat{x}_6$

Meas. Time	1s(1D)	2s(1D1P)	3s(2D)	3s(3D)	3s(2D1P)
0 min.	25000	25000	25000	25000	25000
0.5	24880	12190	4420	3500	508
1.0	24750	11830	280	300	508
1.5	24460	11590	295	205	451
2.0	24050	11360	286	230	411
2.5	23570	11190	295	257	397
3.0	23160	10950	325	285	393
3.5	22840	10660	350	310	386
4.0	22550	10380	376	335	374
4.5	22400	10170	400	360	363
5.0	22320	9710	426	386	352

Figure 5, Comparison of range R2 between with estimation
and without estimation.
(20 % measurment noise, average of 15 runs.)

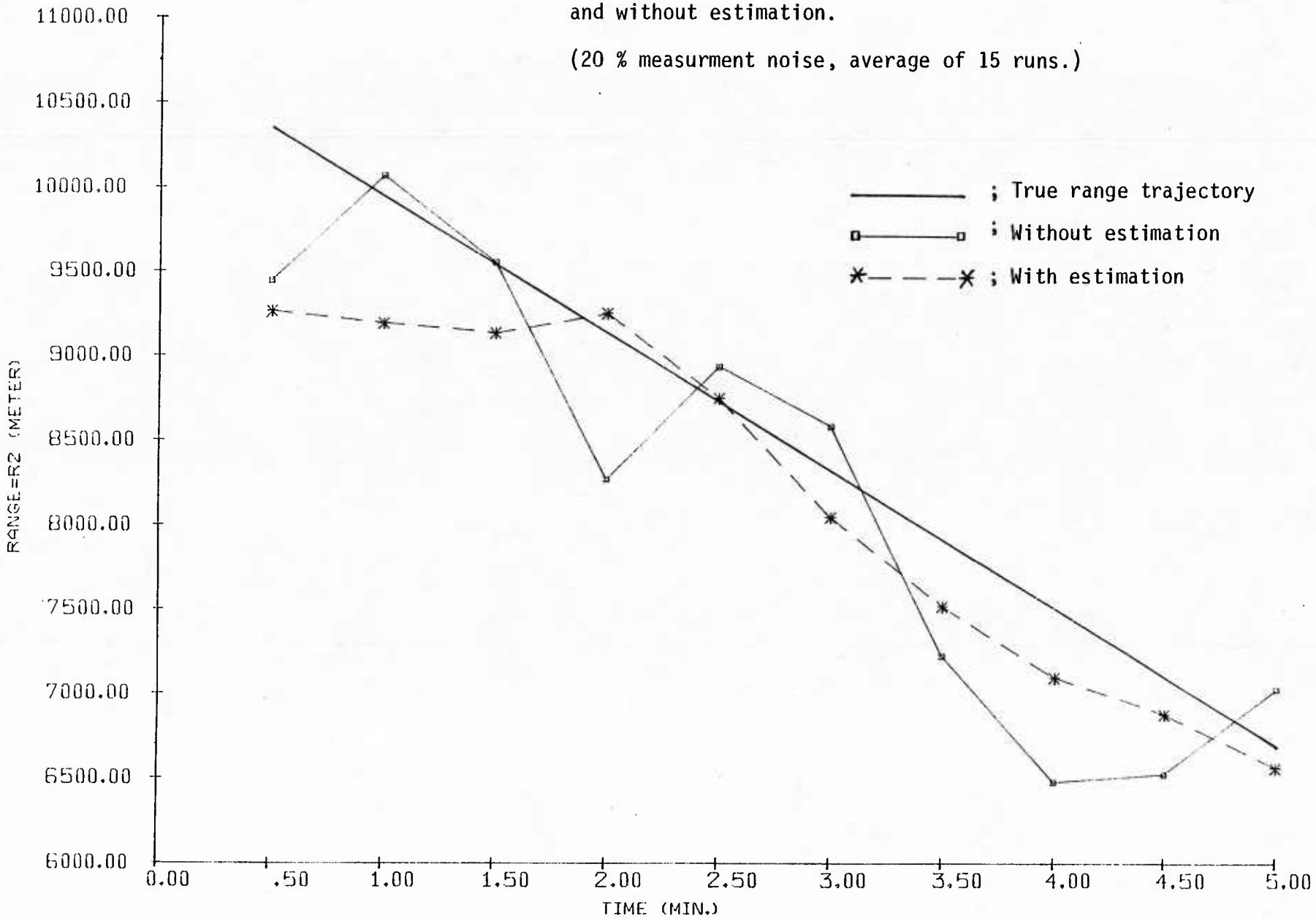

Figure 6, Range R2 without estimation for different measurment noise level. (Average of 15 runs.)

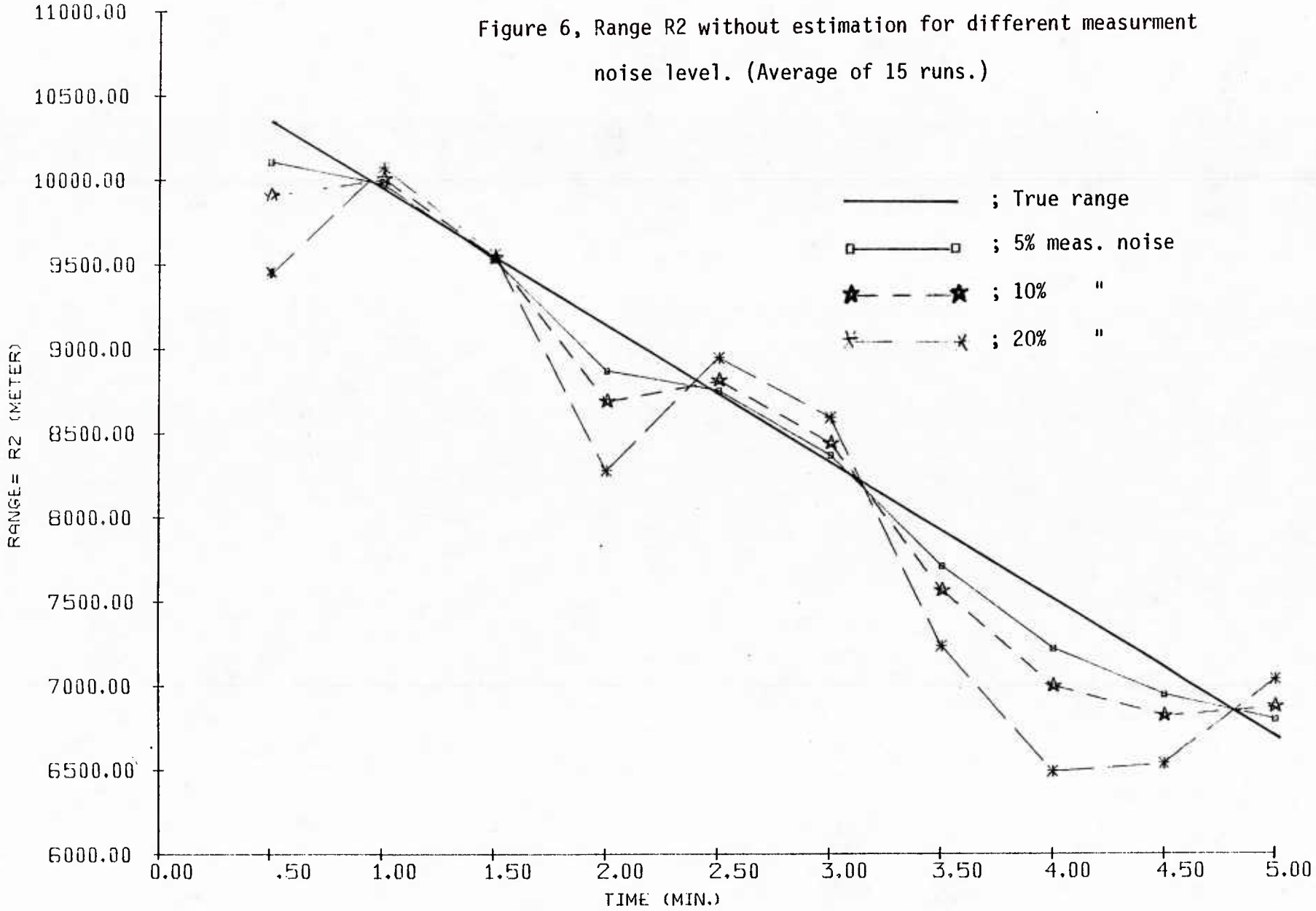

Figure 7, Range R2 with estimation

(Average of 15 runs)

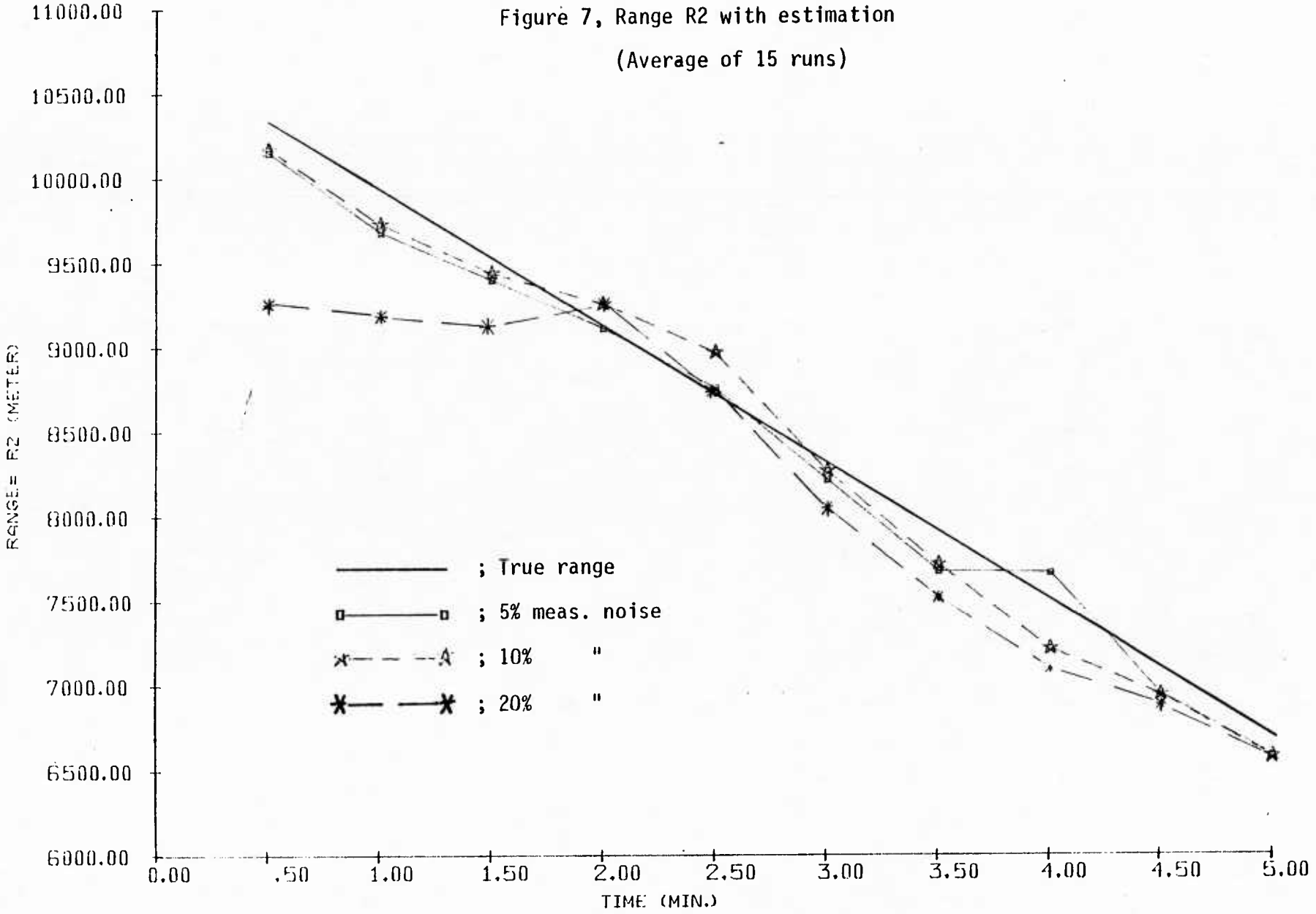

7.0 CONCLUSIONS AND FURTHER RESEARCH

Acoustic wave velocity estimation in the ocean as a means of estimating other target information - target location and its velocity is investigated in this report.

Since the ocean medium is inhomogeneous in depth and in the horizontal plane, wave propagation varies according to the many factors. Most important factors are temperature, depth, salinity and range. Here, the sound velocity is considered as a state variable, which can be estimated from time delay and/or Doppler shift measurements.

The number of sensors and deployment configurations affect the observability of the system. The information rate grows very fast when the measurement includes Doppler shift (2s(1D1P), 3s(2D1P)). The observability test of the nonlinear system shows that when only one sensor is used, the system is totally unobservable during the first five-minute observing period. When two or three sensors are used, the system is observable after one or two measurements, but with different degrees of observability, depending on the measurement policy. Observability of the system with 3s(2D1P) is stronger than any other measurement policy.

The system model is linear but the measurement equation is highly nonlinear, so the measurement equation is linearized and the EKF is utilized. Several variations of the EKF were tried. Since the measurement equation is so complicated, the approximated expression with no iteration shows the best estimation performance. With this scheme, the sound speed along the range of the system was estimated. The 3s(2D1P) measurement shows the best estimation performance as expected. Actual estimation error with this policy is within $\pm$ 5 m/s of 1500 m/s, the assumed true velocity, but with one or two sensors, the estimation error was larger than 25 m/s within a observed period.

With the 2D1P measurement equation and acoustic velocity estimation, the performance for tracking a target is compared with the nonestimation case. As the noise level increases, tracking performance of the estimated case becomes superior to the nonestimated case.

The assumption made here is that the acoustic wave travels through a direct path between target and sensors. In actual inhomogeneous ocean mediums, however, this is not true. The wave propagating along the several modes depends on the source depth. By applying ray theory or the well known Snell's law, sound velocity can be estimated more accurately. Including these theories in the estimation algorithm does not present any great difficulty. However, this is the topic for future research. Then, with this more exact sound speed, more accurate target position and its velocity estimates may be computed which is the final objective of this research.

8.0 REFERENCES

1. Robert A. Helton, "Oceanographic and Acoustic Characteristics of the Dabob Bay Range - Report 1300," Naval Torpedo Station, Keyport, WA, November 1976.

2. D.L. Alspach, G.L. Mohnkern and R.N. Lobbia, "Sound Speed Estimation as a Means of Improving Target Tracking Performance," AD-A086, 603/8, ORINCON Co., La Jolla, CA, 1980.

3. D.L. Alspach and R.N. Lobbia, "A Case Study in Adaptive Sound Speed Estimation," AD-A086, 605/3, ORINCON Co., La Jolla, CA, 1980.

4. W.F. Denham and S. Pines, "Sequential Estimation When Measurement Function Nonlinearity is Comparable to Measurement Error," AIAA J. 4, No. 6, 1966.

5. A.H. Jazwinski, Stochastic Process and Filtering Theory, Academic Press, New York, 1970.

6. A.V. Oppenheim, et al., Application of Digital Singal Proc., Prentice Hall, Inc., 1978.

7. R.J. Urick, Principles of Underwater Sound, 2nd ed., McGraw-Hill, New York, 1975.

8. Yu. M.L. Kostyukovskii, "Obervability of Nonlinear Controlled Systems," Automat. Remote Contr. 9, pp. 1384-1396, 1968.

9. Yu. M.L. Kostyukovskii, "Simple Conditions of Observability of Nonlinear Controlled Systems," Automat. Remote Contr. 10, pp. 1575-1584, 1968.

10. T.J. Tarn, et al., "Observability of Nonlinear Systems," Information & Control 22, pp. 89-99, 1973.

11. E.W. Griffith and K.S.P. Kumar, "On the Observability of Nonlinear Systems I," J. Math. Anal. Appl. 35, pp. 135-147, 1971.

12. J.M. Fitts, "On the Observability of Nonlinear Systems with Application to Nonlinear Regression Analysis," Information Sciences 4, pp. 129-156, 1972.

13. T. Fujisawa and E.S. Kuh, "Some Results on Existence in Uniqueness of Solution of Nonlinear Network," IEEE Trans. Circuit Theory CT-18, No. 5, pp. 501-506, 1971.

14. Uwe Schoewandt, "On Observability of Nonlinear Systems," Prague Sym. Inden. and Para. Estim., 1970.

15. S.C. Nardone, and V.J. Aidala, "Observability Criteria for Bearing-Only Target Motion Analysis," IEEE Trans. Aero. Elect. Sys. AES-19, No. 2, pp. 162-166, March 1981.